INTEGRATED MULTI-PHYSICS WORKFLOW FOR GEOTHERMAL EXPLORATION IN TURKEY

Federico Ceci[1]

[1] Schlumberger, Via Clericetti 42/A 20133 Milan, Italy

fceci@slb.com

Keywords: Integration, MT, Turkey.

ABSTRACT

The magnetotelluric method (MT) provides useful information regarding the geologic, compositional and hydraulic conditions of geothermal systems, through imaging of the electrical resistivity in the subsurface. Thanks to the broadband frequency content of the MT measurements and to the diffusive nature of the EM field in the earth, the MT method allows to reach high depths at low frequencies, while keeping good resolution of the shallow section; on the other hand, cultural noise can severely affect the results of MT soundings, and dedicated, robust processing procedures must be implemented. In the presented case study, data-driven MT modelling results were analysed, in an integrated framework, together with geologic data to maximize the chance of success of a geothermal exploration campaign in West Anatolia, Turkey.

1. INTRODUCTION: THE GEOLOGIC CONTEXT

Turkey is one of the most seismically active regions in the world. Its geological and tectonic evolution has been dominated by the repeated opening and closing of the Paleozoic and Mesozoic oceans (Dewey and Sengör, 1979) and it is located within the Mediterranean Earthquake Belt whose complex deformation results from the continental collision between the African and the Eurasian plates. Southern and northern parts of Turkey are bordered by the East Anatolian Fault Zone (EAFZ) and by the North Anatolian Fault Zone (NAFZ), respectively. Those tectonically-active borders are marked by young volcanics and active faults, the latter allowing circulation of heat-generating hot springs. The distribution of those hot-water manifestations in Turkey is roughly parallel to the distribution of fault systems, young volcanism and hydrothermally altered areas (Simsek, 1997) (Figure 1).

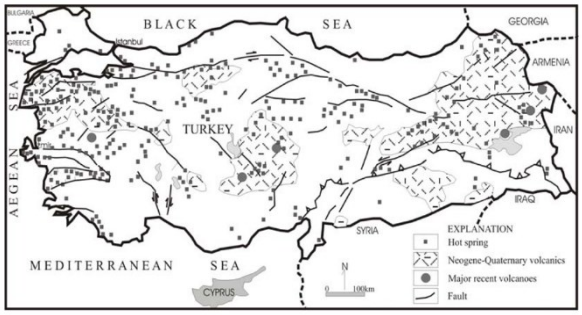

Figure 1: Simplified main neotectonic lines and hot spring distribution of Turkey (from Simsek, 1997 and Baba et al., 2008).

There is a total of about a thousand thermal and mineral water spring groups in Turkey (Baba and Özcan, 2005). In particular, in the western part of Turkey, one of the most important geothermal regions is the Peninsula of Biga characterized by an anomalously high heat flow that has developed as a result of crustal thinning in an area of tectonic extension, in association with continental convergence. This area is closely related to the active tectonic zones of the North Anatolian Fault Zone and West Anatolian Graben Systems. For this reason, geothermal systems manifest themselves with several hot-water springs (Tuzla, Kestanbol and Hıdırlar are geothermal fields within the Biga Peninsula). This geologic setting makes the Anatolian Peninsula one of the most promising areas for geothermal exploration.

2. WORKFLOW

The MT method is based upon the measurement of the fluctuations of the natural EM field at the earth's surface over a wide frequency range (10^{-3} to 10^{4} Hz). The method is extensively applied to geothermal exploration thanks to its high depth of investigation (~several km), versatile acquisition logistics and its cost-effectiveness, if compared to seismic acquisition. The main drawback of the methodology, is the noise with anthropic origin that can severely affect and even compromise the quality of MT soundings. Due to this dedicated and robust processing procedure, must be implemented in order to ensure the success of the MT modelling stage. In the presented case scenario, a total of 211 MT stations was acquired in 2017; the magnetotelluric soundings were recorded along a series of 2D profiles approximately oriented SW-NE. A

legacy survey was conducted in the same area, partially overlapping with the 2017 sites; additional 20 MT legacy sites were included during the 2017 modelling phase, as infill to the new survey. The MT data acquired during the most recent campaign were treated using robust processing techniques with the objective of enhancing the signal-to-noise ratio particularly for the magnetic transfer function (tipper), which showed poor quality after the non-robust original processing (Figure 2).

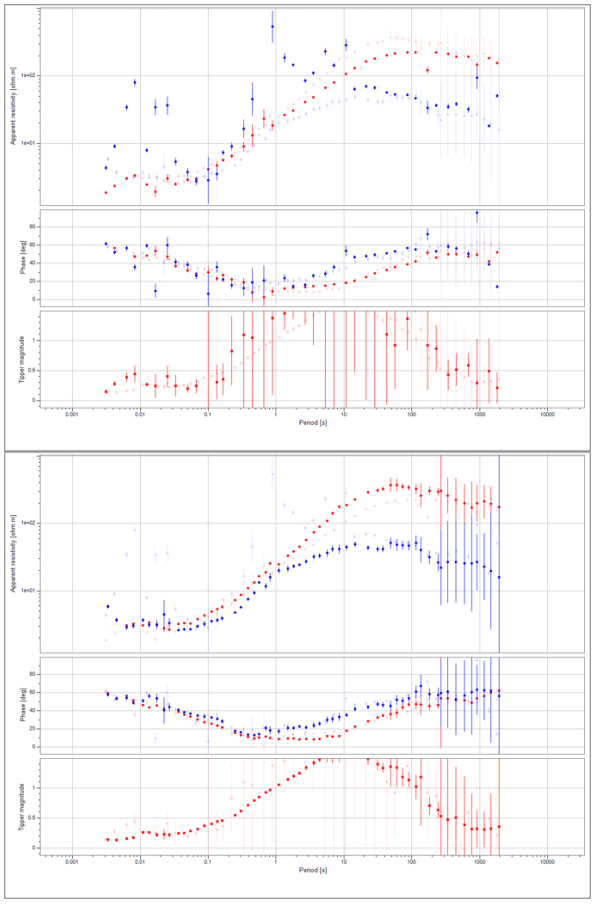

Figure 2: Positive effect of data processing with robust algorithm on a site affected by cultural noise. Top- non-robust processing, Bottom – robust processing results. Data rotation is N0°E

2.1 Data preconditioning and modelling workflow

Data quality varied over the survey area, following the different distribution of human settlements: the central zone of the area, close to the coast, were affected by local noise sources due to anthropic activities, while at the borders the data quality was better. The natural MT signal was highly variable during the acquisition period, due to the fluctuating solar activity. Prior to the inversion step, data was quality controlled, to remove outliers and distorted data-points. Particular care was given to the tipper component, that for some sites showed an inconsistent behavior with respect to the rest of the survey data. Because no prior geologic information was adopted in the modelling phase, data points showing strong distortion (e.g. off-quadrant impedance phase/extreme value of tipper magnitude), possibly due to regional features absent in the starting model, were muted, to prevent the insertion of unrealistic artifacts in the resulting or final resistivity model.

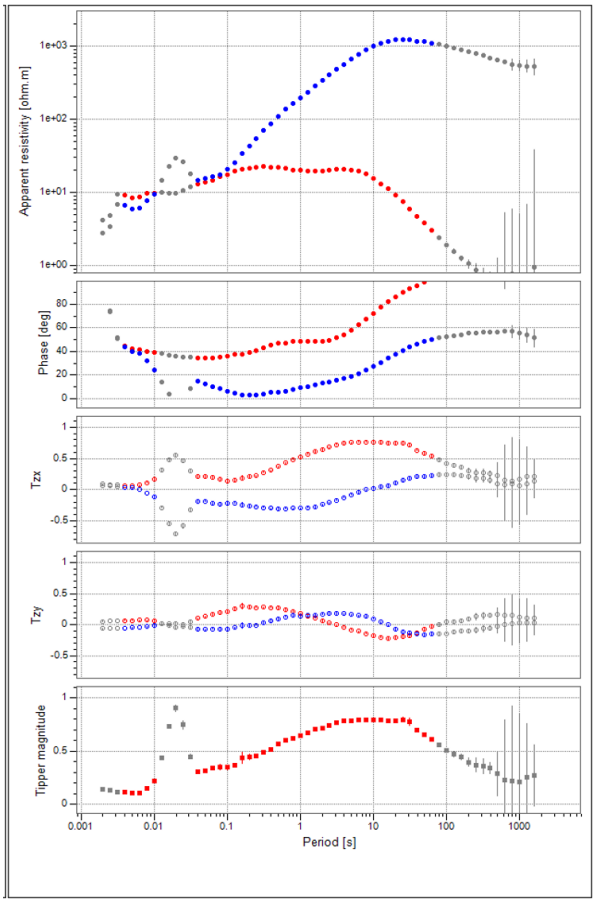

Figure 3: Example of data muting: greyed points are removed from the inversion procedure. Data rotation is N73°E

To assess the quality of the dataset, apparent resistivity and phase maps at a constant frequency were produced and checked, also against know prior information. The analysis showed the consistency of the two merged datasets (2017 and legacy), together with a good lateral continuity of the soundings (Figure 4).

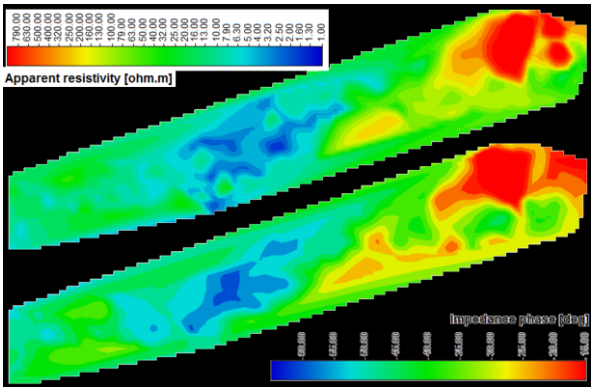

Figure 4: YX Apparent resistivity (Top) and impedance phase (Bottom) maps extracted at 0.1Hz and 1Hz, respectively. Data rotation is N73°E.

Apparent resistivity and phase pseudo-sections were also produced, following the 2D profiles defining the

survey layout. The inspection of the pseudo-sections revealed the presence of a deep resistive feature – with good lateral continuity – overlaid by a shallower resistive/conductive transition (Figure 5).

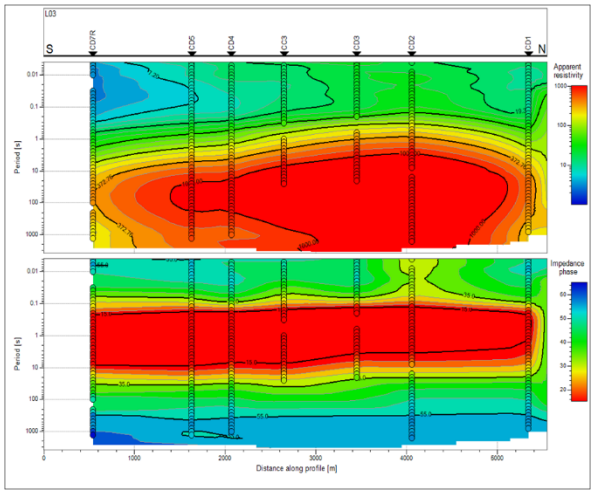

Figure 5: Apparent resistivity and impedance phase pseudo-sections of YX component along a receiver line. Data rotation is N73°E

2.2 3D modelling results and integration

The full impedance tensor was inverted with the algorithm described by Andreasi and Masnaghetti, 2015. The inversion started from a uniform resistivity distribution of 10 Ωm, including high-resolution topography and bathymetry. The seawater layer was included in the starting resistivity distribution. The final model inverted the frequency band from 100Hz to 0.002Hz, with 10 frequencies per decade, thus using a total of 47 frequencies. During the inversion, error floors of 5% were used for lnZxy and lnZyx, and 10% for Zxx/yy, while an absolute error floor of 0.01 was adopted for the Tipper.

The inversion converged to a geologically plausible resistivity distribution, matching the general geologic trend of the area and producing also a low level of data misfit. Consistently with the data, the model showed a laterally variable increase of resistivity at depth gently dipping towards SW, in agreement with the QC performed by visual inspection of apparent resistivity and phase maps, and demonstrating that the resistivity distribution recovered from the inversion was honored by the data. (Figure 6).

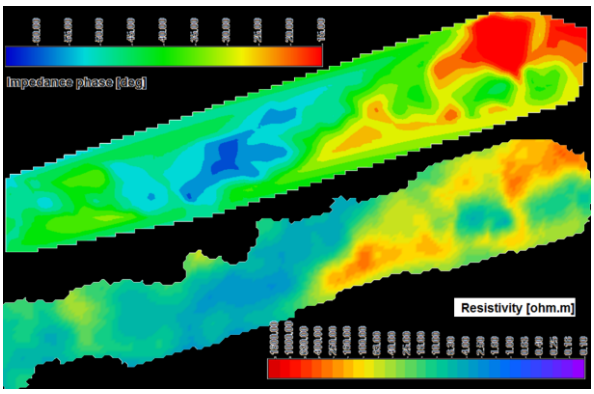

Figure 6: YX impedance phase map at 1 Hz (Top) and resistivity slice from 3D model extracted at 500m depth (Bottom). Data rotation is N73°E

The final 3D resistivity model, although obtained from purely data-driven modelling, showed a good level of consistency with the general geologic settings of the area: shallow lateral resistivity variations congruous with the surface geology and a deep, resistive body, delineating the graben's shoulders, overlaid by a more conductive layer, marking the later sedimentary filling (Figure 7).

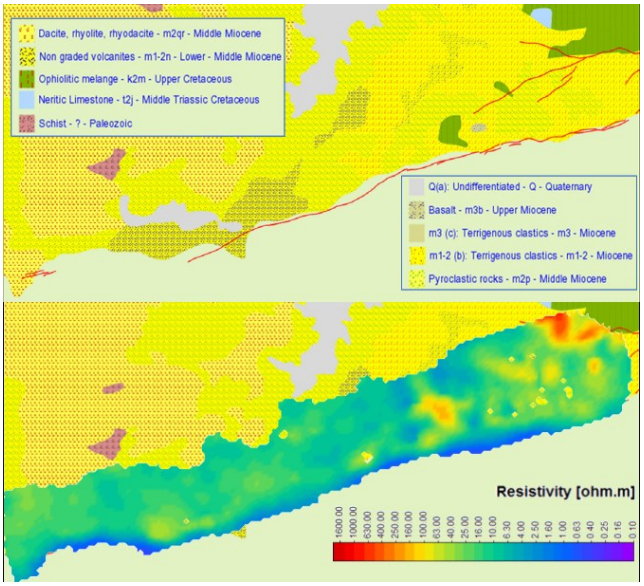

Figure 7: Surface geology map (Top) and resistivity slice from 3D model extracted at 0m depth (Bottom).

Resistivity slices at different depths allowed to follow the vertical and lateral resistivity variations of the subsurface and their correlation with the expected geologic features (Figure 8).

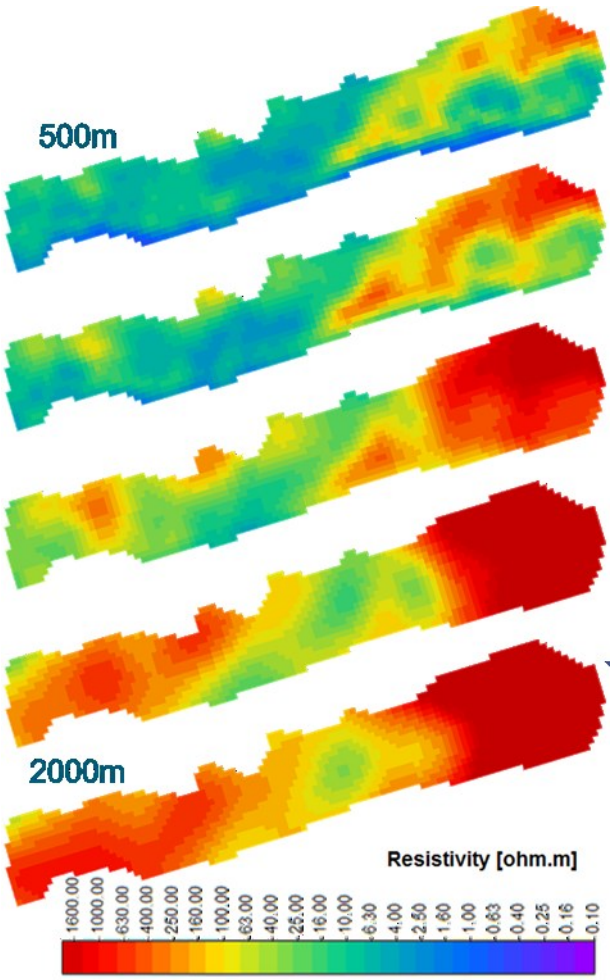

Figure 8: Resistivity slices from 3D model extracted at increasing constant depth, from 500m (Top) to 2000m below topography (Bottom).

Lateral resistivity variations mapped by the 3D resistivity model could either represent a differential subsidence due to a more segmented and compartmentalized sedimentary basin, or an actual upwelling feature related to an active geothermal field.

3D resistivity distribution from unconstrained modelling can be adopted as guidance to map the main geologic features of the area; the deep resistor at depth can be considered as an indication of the geometry of the geoelectrical basement. Integrated interpretation of the resistivity model, incorporating prior knowledge, such as surface and or regional geology, allowed to interpret general structural features, helping the comprehension of the subsurface. Using a iso-resistivity surface as guidance, an approximate position of the geoelectrical basement can be interpreted, as displayed in Figure 9, Top.

As expected in this type of tectonic setting and as observed in other geothermal fields in Turkey, the current extensional regime is superimposed to an earlier strain field roughly perpendicular to the current one: this interference generates preferential paths for the geothermal fluid upwelling from deep sources to the shallower reservoirs. This concept seems to be represented in the NS section reported in Figure 9, where extensional faults perpendicular to the main tectonic trend can be inferred from the resistivity model (light blue solid line). The availability of a 3D model allows to extract structural information (i.e. fault geometry) in a 3D sense; the correlation of the information resulting from the MT modelling stage with the available geologic knowledge is a valuable tool for the geothermal exploration campaigns, where structural information from seismic imaging is seldom available.

Well data were also available in the area, in terms of lithology analysis. The resistivity distribution from the MT unconstrained modelling was extracted along the trajectory of the well and compared with the well data. The trend of the resistive column matched the stratigraphic column, correlating outcropping volcanic formations with a high resistivity value, Miocene shale layers with a conductor, and deep volcanic formations at the Mesozoic/Paleozoic level with the recovered deep resistor.

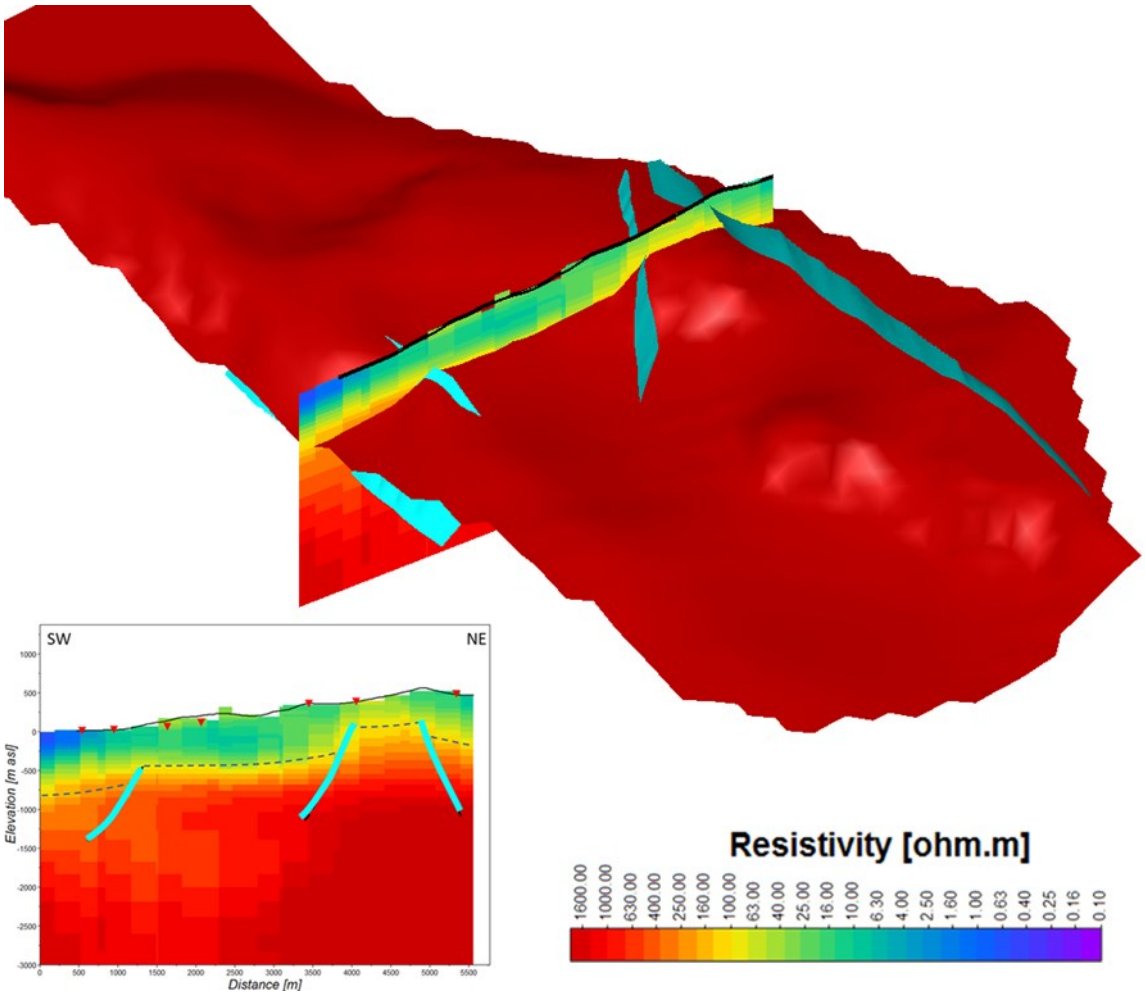

Figure 9: 3D view of the geoelectrical basement interpreted from MT data (dark red surface) and trace of the extensional faults (cyan planes). SW-NE section reported on the bottom shows the resistivity model with structural interpretation of the basement (dashed line) and extensional faults (cyan solid lines).

3. CONCLUSIONS

Integrated interpretation of the results of unconstrained MT 3D modelling indicate the presence of a strong, deep resistive body compatible with the expected geoelectrical basement of the area. Resistivity-guided structural interpretation carried out in the area matched prior geologic information and allowed to track structural features of the subsurface. Comparison with lithology extracted from a well within the survey showed a consistency between the data-driven resistivity distribution and the geology, thus increasing the confidence on the obtained results. Having a geophysical methodology able to quickly identify main tectonic features is crucial to focus the attention and then locate the most promising geothermal prospects and make sound decisions in terms geothermal wells drilling.

REFERENCES

Baba, A., and Özcan, H: Monitoring and evaluation of the geothermal fluid on soil and water in Tuzla geothermal field by GIS. In: Erasmi, S., Cyffka, B., and Kappas, M. (Ed.), 138-143, Remote sensing and GIS for environmental studies, Göttinger Geographische Abhandlungen, vol. 113, Göttingen, (2005)

Dewey, J.F., and Sengör, A.M.C. Aegean and surrounding regions: complex multiplate and continuum tectonics in a convergent zone. *Geological Society of America Bulletin*, I-90, (1979), 84–92.

Golfré Andreasi, F. and Masnaghetti, L. *Decoupled Model Grids for Simultaneous Joint Inversion of MT and CSEM Data*. 77th EAGE Conference and Exhibition, (2015), Extended Abstracts N105

Simsek, S. Geothermal potential in northwestern Turkey. In: Schindler, C., and Pfister, M. (Ed.),111-123, Active Tectonics of northwestern Anatolia. The Marmara Poly-Project. Vdf Hochschulverlag AG an der ETH, Zurich, (1997)